2019

Crystal structure, magnetism and magnetocaloric properties of $Mn_{2-x}Sn_{0.5}Ga_{0.5}$ (x=0, 0.3, 0.5, 0.8) alloys

H. Qian

Rabindra Pahari

K. Schroeder

Shah R. Valloppilly

Y. Huh

See next page for additional authors

Authors

H. Qian, Rabindra Pahari, K. Schroeder, Shah R. Valloppilly, Y. Huh, Pavel V. Lukashev, J. Hu, Parashu Kharel, and David J. Sellmyer

Crystal structure, magnetism and magnetocaloric properties of $Mn_{2-x}Sn_{0.5}Ga_{0.5}$ (x=0, 0.3, 0.5, 0.8) alloys

H. Qian,[1,2] R. Pahari,[3] K. Schroeder,[2] S. Valloppilly,[4] Y. Huh,[2] P. Lukashev,[5] J. Hu,[1] P. Kharel,[2] & D. J. Sellmyer[3,4]

1 School of Materials Science and Engineering, Changzhou University, Changzhou, China
2 Department of Physics, South Dakota State University, Brookings, SD 57007, United States
3 Department of Physics and Astronomy, University of Nebraska, Lincoln, NE 68588, United States
4 Nebraska Center for Materials and Nanoscience, University of Nebraska, Lincoln, NE 68588, United States
5 Department of Physics, University of Northern Iowa, Cedar Falls, IA 50614, United States

Corresponding author — P. Kharel, *email* parashu.kharel@sdstate.edu

Abstract

Magnetic refrigeration based on the magnetocaloric effect has attracted recent attention due to advantages such as high efficiency and environmental friendliness. We have investigated the structural, magnetic and magnetocaloric properties of $Mn_{2-x}Sn_{0.5}Ga_{0.5}$ (x=0, 0.3, 0.5, 0.8) alloys prepared using arc-melting

Published in *Journal of Magnetism and Magnetic Materials* 471 (2019), pp 411–415
doi:10.1016/j.jmmm.2018.09.123

Submitted 10 July 2018; revised 28 August 2018; accepted 30 September 2018; published 1 October 2018.

and meltspinning techniques with prospects for magnetic refrigeration. The $Mn_{2-x}Sn_{0.5}Ga_{0.5}$ alloys, except for $Mn_{1.2}Sn_{0.5}Ga_{0.5,}$ have a single-phase hexagonal crystal structure. The $Mn_{1.2}Sn_{0.5}Ga_{0.5}$ alloy also contains a small amount of $MnSn_2$ impurity phase. The Curie temperature and high-field (30 kOe) magnetization at 55 K decrease with increasing Mn concentration from 306 K and 64.1 emu/g (1.07 μ_B/Mn) for $Mn_{1.2}Sn_{0.5}Ga_{0.5}$ to 262 K and 46.7 emu/g (0.85 μ_B/Mn) for $Mn_2Sn_{0.5}Ga_{0.5}$, respectively. The peak values of magnetic entropy change are relatively small with $\Delta S_{M,max}$=1.7 $Jkg^{-1}K^{-1}$ for $Mn_{1.5}Sn_{0.5}Ga_{0.5}$ at 30 kOe. Despite this, these materials show considerable relative cooling power (RCP) along with a wide working temperature range near room temperature and negligible magnetic and thermal hysteresis, where $Mn_{1.2}Sn_{0.5}Ga_{0.5}$ shows a highest RCP of 102.3 Jkg^{-1} at 30 kOe.

1. Introduction

Magnetic materials exhibiting robust magnetocaloric effect (MCE) have attracted increasing attention recently because of their potential for emerging magnetic refrigeration (MR), a promising substitute for the conventional vapor compression cooling technology [1–6]. The MR uses solid-state magnetic materials as refrigerants and presents negligible environmental hazards [3]. The cooling effect in MR is achieved by magnetization and demagnetization of magnetocaloric materials and the process can be dissipation free in the case of soft ferromagnetic materials resulting in 100% of the Carnot efficiency [7]. The current vapor-compression-based refrigerators have a maximum efficiency of about 40%, whereas the prototype MR devices have shown up to 60% of the Carnot efficiency [8]. In addition to excellent MCE, the magnetocaloric materials need to meet other requirements such as high electrical resistance, high thermal conductivity, low heat capacity, mechanical stability, safe constituent elements and high chemical stability [8]. The main challenge is to find suitable solid-state magnetic materials exhibiting these properties with a wide working-temperature range near room temperature.

For near-room-temperature MR, Gd and Gd-based alloys have been extensively investigated [9,10]. However, the high price and susceptibility to oxidation restrict the use of Gd and its alloys in commercial cooling devices [11]. Other materials showing large MCE include $La(Fe_{1-x}Si_x)_{13}$, $MnFeP_xAs_{1-x}$ and $Ni_{2-x}Mn_{1-x}Ga$ Heusler alloys [12–17]. Some of these materials produce a giant entropy change at the temperatures of their magnetostructural phase transitions but the large

thermal and magnetic hysteresis and narrow working temperature range limit their usefulness in commercial MR devices [3,8]. Oxide materials such as $R_{1-x}A_xMnO_3$ (R=lanthanide and A=divalent alkaline earth) are other prospective materials for room temperature MR applications because some of these materials exhibit magnetic phase transitions near room temperature, use non-toxic and relatively cheap elements and are chemically stable [8,18,19]. The only issue with these materials is their low thermal conductivity and relatively low cooling efficiency as compared to Gd-based materials [3,20].

Our interest is to synthesize and investigate Mn_2Ga-based materials exhibiting second order magnetic phase transitions near room temperature, because these materials are earth-abundant, non-toxic, and their structural and magnetic properties can be modified as desired by adjusting elemental compositions [21,22]. The materials exhibiting second order phase transition are free from the magnetic and thermal hysteresis, which can help in increasing the operation frequency of refrigeration devices. In addition, the atomic magnetic moment in compounds containing Mn is much higher than that in compounds containing Ni, Co or Fe, which in some compounds reach up to 4 μ_B/Mn [23]. Since MCE scales with the size of magnetic moment, Mn-based compounds have been investigated as potential rare-earth-free magnetocaloric materials [24]. Here, we report our experimental investigation on Sn substituted Mn-Ga alloys, namely, $Mn_{2-x}Sn_{0.5}Ga_{0.5}$ (x=0, 0.3, 0.5, 0.8) and show that the saturation magnetization, Curie temperature (T_C) and peak value of entropy change can be tuned by adjusting the Mn concentration without any change in the crystal structure. A partial substitution of Ga with Sn in Mn-Ga alloys has reduced their T_C to temperatures near 300 K, as desired for room temperature MR applications.

2. Experimental methods

In order to investigate the crystal structure and magnetocaloric properties of Sn substituted Mn_2Ga-based compounds, we have prepared a series of compounds $Mn_{2-x}Sn_{0.5}Ga_{0.5}$ (x=0, 0.3, 0.5, 0.8) in the form of ribbons using arc melting and rapid quenching in a meltspinner. First, small pieces of Mn, Sn and Ga with the proper weight ratio

were cut from commercially available pellets and melted on a water-cooled Cu hearth of an arc-melting furnace in a highly pure argon environment. All these used elements were at least 99.95% pure. In order to remove the oxide layer present in the commercial Mn pieces, they were first melted into an ingot and the surface was cleaned with sand paper before using it in alloy preparation. The arc-melted alloy ingots were broken into pieces, induction melted in a quartz tube inside a melt-spinner chamber and rapidly quenched onto the surface of a copper wheel rotating at 25 m/s. We used a quartz tube with nozzle diameter of 0.66mm positioned at 5mm above the surface of the wheel. A RF power of 2100W and an ejection pressure of 200 mbar were used. The crystal structures of the samples were investigated using powder X-ray diffraction (XRD) in a Rigaku MiniFlex600 diffractometer with copper Kα radiation. The scan rate was 2 degrees per minute. The XRD patterns were analyzed by Rietveld method using TOPAS software (Bruker, AXS). The magnetic properties were investigated using a Quantum Design VersaLab magnetometer. The estimated elemental compositions were confirmed using energy-dispersive X-ray spectroscopy (EDX) in a FEI Nova NanoSEM450. The measured compositions are $Mn_{1.2}Sn_{0.5}Ga_{0.5}$, $Mn_{1.5}Sn_{0.5}Ga_{0.5}$, $Mn_{1.7}Sn_{0.5}Ga_{0.5}$ and $Mn_2Sn_{0.5}Ga_{0.5}$ with a 0.1% error in the measurement. The crystal and magnetic structures of $Mn_2Sn_{0.5}Ga_{0.5}$ were also confirmed with standard density functional calculations.

3. Results and discussion

The XRD patterns of the rapidly quenched $Mn_{2-x}Sn_{0.5}Ga_{0.5}$ (x=0, 0.3, 0.5, 0.8) ribbons recorded at room temperature are shown in **Fig. 1**. The XRD patterns were recorded on powder samples ground from $Mn_{2-x}Sn_{0.5}Ga_{0.5}$ ribbons. The XRD patterns are indexed with the hexagonal crystal structure (space group $P6_3/mmc$). In order to determine the lattice parameters and the presence of secondary phases, the experimental XRD patterns were compared with the patterns simulated using Rietveld method. $Mn_{2-x}Sn_{0.5}Ga_{0.5}$ samples are found to be formed with $Co_{1.75}Ge$-prototype structure, where Mn atoms occupy 2a (0, 0, 0) and 2d (1/3, 2/3, 3/4) sites and Sn and Ga share 2c (1/3, 2/3, 1/4) [25]. The 2d sites are conceived as “interstitial sites” where

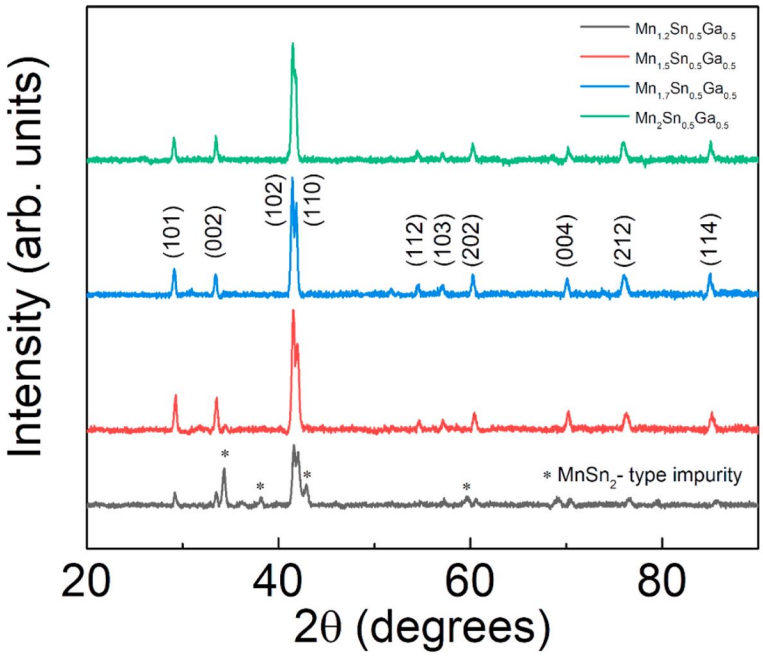

Fig. 1. The room-temperature powder XRD patterns of the as-quenched $Mn_{2-x}Sn_{0.5}Ga_{0.5}$ (x=0, 0.3, 0.5, 0.8) ribbons.

the partial occupation of this sites is most probable. Rietveld analysis indeed shows that the site occupation of Mn at the 2d site progressively decreases with increasing *x* (decreasing Mn content). The lattice parameters obtained from the Rietveld analysis are: *a*=4.304 Å, 4.322 Å, 4.331 Å, and 4.340 Å, and *c*=5.346 Å, 5.375 Å, 5.379 Å and 5.370 Å for $Mn_{1.2}Sn_{0.5}Ga_{0.5}$, $Mn_{1.5}Sn_{0.5}Ga_{0.5}$, $Mn_{1.7}Sn_{0.5}Ga_{0.5}$ and $Mn_2Sn_{0.5}Ga_{0.5}$, respectively. The increase in lattice parameters both *a* and *c*, suggests the unit cell expansion as a function of increasing Mn and this observation is consistent with the Rietveld analysis that Mn progressively occupy the 2d site and may cause gradual expansion of the lattice. The XRD analysis also suggested that $Mn_{1.2}Sn_{0.5}Ga_{0.5}$ contains a small amount of $MnSn_2$-type impurity phase. $Mn_{2-x}Ga$ alloys have been synthesized in the hexagonal, tetragonal ($L1_0$), and tetragonal ($D0_{22}$) structures but the hexagonal structure is not the most stable structure [26]. The partial replacement of Ga with Sn in $Mn_{2-x}Ga$ helped to stabilize the hexagonal structure.

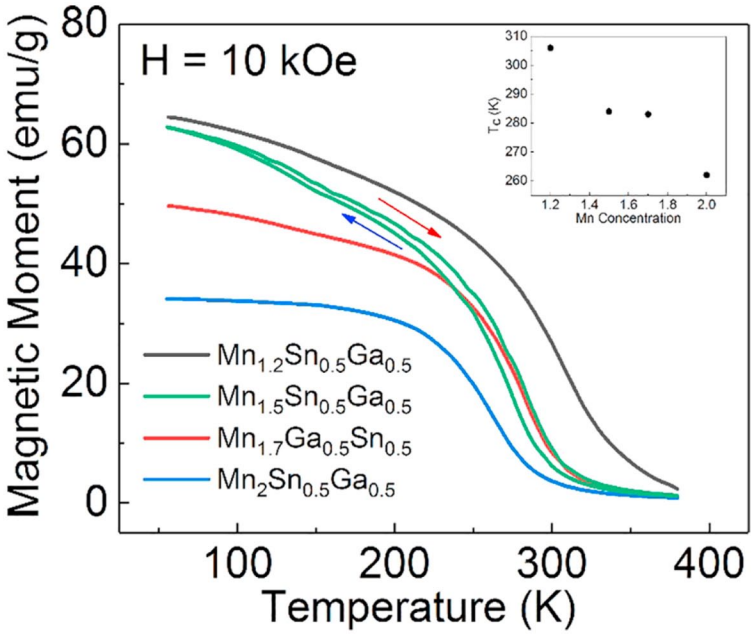

Fig. 2. Thermomagnetic curves of as-quenched $Mn_{2-x}Sn_{0.5}Ga_{0.5}$ (x=0, 0.3, 0.5, 0.8) ribbons, the inset shows the T_c as a function of Mn concentration.

Fig. 2 shows the thermomagnetic curves *M(T)* of the rapidly quenched $Mn_{2-x}Sn_{0.5}Ga_{0.5}$ (x=0, 0.3, 0.5, 0.8) ribbons between 55 K and 380 K. The *M(T)* curves were recorded at 10 kOe while the temperature was increased above 55 K. All samples show smooth *M(T)* curves with single magnetic phase transitions at their respective Curie temperatures. The *M(T)* was also measured while cooling the samples from 380 K to 55 K and no thermal hysteresis was observed. The Curie temperatures determined from peak point of the first derivative of the *M(T)* curves vary almost linearly with Mn concentration in $Mn_{2-x}Sn_{0.5}Ga_{0.5}$, where the T_C for $Mn_{1.2}Sn_{0.5}Ga_{0.5}$, $Mn_{1.5}Sn_{0.5}Ga_{0.5}$, $Mn_{1.7}Sn_{0.5}Ga_{0.5}$ and $Mn_2Sn_{0.5}Ga_{0.5}$ are respectively 304 K, 284 K, 283 K and 262 K, see the inset of Fig. 2 [27]. Further, the low-temperature (50 K) magnetization also increases with decreasing Mn concentration in $Mn_{2-x}Sn_{0.5}Ga_{0.5}$. The increase in both the Curie temperature and low-temperature magnetization with the decrease in Mn concentration suggest that there is a ferrimagnetic order between partially compensating Mn moments located on the two crystallographically different sites of hexagonal crystal lattices of the $Mn_{2-x}Sn_{0.5}Ga_{0.5}$ alloys [26].

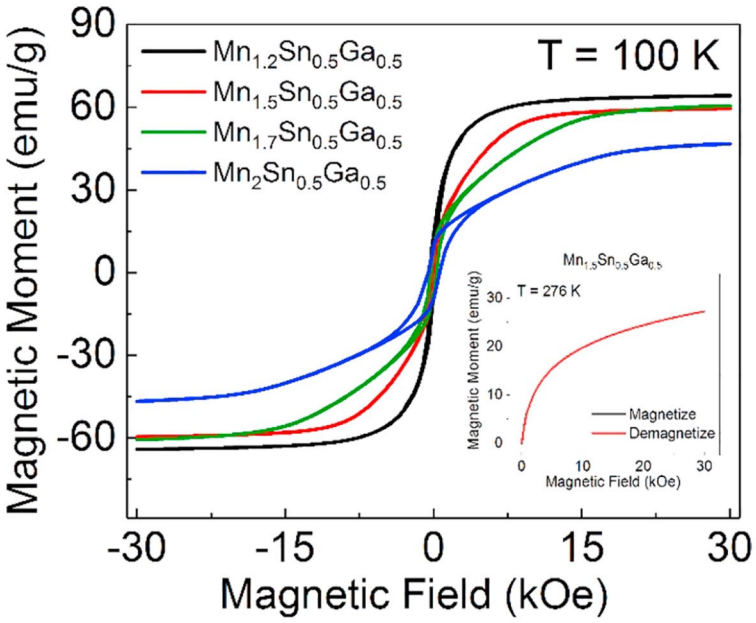

Fig. 3. Isothermal magnetization *M(H)* curves of as-quenched $Mn_{2-x}Sn_{0.5}Ga_{0.5}$ (x=0, 0.3, 0.5, 0.8) ribbons.

Fig. 3 shows the magnetic field dependence of magnetization *M(H)* for as-quenched $Mn_{2-x}Sn_{0.5}Ga_{0.5}$ (x=0, 0.3, 0.5, 0.8) ribbons recorded at 100 K. The *M(H)* loops of all the samples are nearly saturated at 30 kOe. However, the magnetic field required to saturate *M(H)* loops increases with Mn concentration in $Mn_{2-x}Sn_{0.5}Ga_{0.5}$ indicating that the increased number of Mn atoms in the hexagonal crystal lattice promote the antiferromagnetic alignment of Mn moments. All samples have small coercivities (H_c) but are hard magnetic in nature [28], where the H_c for $Mn_{1.2}Sn_{0.5}Ga_{0.5}$, $Mn_{1.5}Sn_{0.5}Ga_{0.5}$, $Mn_{1.7}Sn_{0.5}Ga_{0.5}$ and $Mn_2Sn_{0.5}Ga_{0.5}$ are respectively 210 Oe, 230 Oe, 290 Oe and 590 Oe. The high-field magnetization increases with the decrease in Mn concentration, from 46.7 emu/g (0.85 μ_B/Mn) for $Mn_2Sn_{0.5}Ga_{0.5}$ to 64.1 emu/g (1.07 μ_B/Mn) for $Mn_{1.2}Sn_{0.5}Ga_{0.5}$. This is also an indication of ferrimagnetic arrangement of Mn moments in the $Mn_{2-x}Sn_{0.5}Ga_{0.5}$ lattice. Although $Mn_{1.2}Sn_{0.5}Ga_{0.5}$ contains a small amount of $MnSn_2$-type impurity phase, the magnetization of the sample is not affected because of the antiferromagnetic nature of $MnSn_2$ with Neel temperature of 324 K [29].

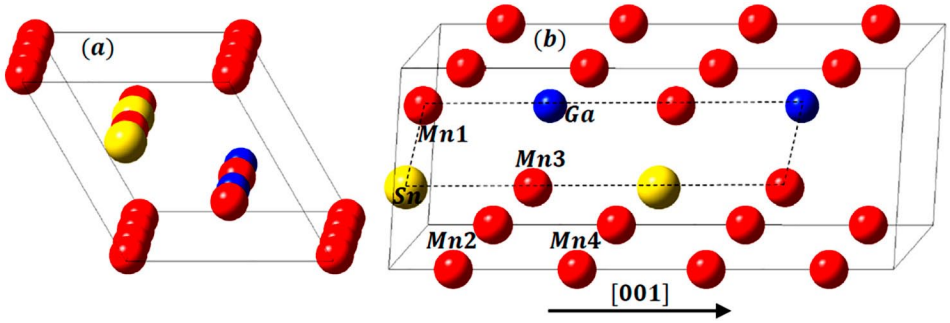

Fig. 4. Fully relaxed atomic structure of $Mn_2Sn_{0.5}Ga_{0.5}$ (top view – (a); side view – (b)). For better visualization, two unit cells are shown in [0 0 1] direction. The atoms are color coded as indicated on the figure.

We also investigated the crystal and magnetic structures of $Mn_2Sn_{0.5}Ga_{0.5}$ using standard density-functional calculations. In particular, we used the projector augmented-wave method (PAW) [30], implemented in the Vienna *ab initio* simulation package (VASP) [31] within the generalized-gradient approximation (GGA) [32]. The integration method [33] with a 0.05 eV width of smearing was used, along with the plane-wave cut-off energy of 500 eV and energy convergence criteria of 10_{-2} meV for atomic relaxation, and 10^{-3} meV for the total energy calculations. **Fig. 4** shows a fully relaxed atomic arrangement of $Mn_2Sn_{0.5}Ga_{0.5}$, in the hexagonal structure. The calculated lattice parameters $a=b=4.37$ Å and $c=5.34$ Å, and the antiparallel arrangement of Mn magnetic moments for $Mn_2Sn_{0.5}Ga_{0.5}$ are in good agreement with our experimental results. The ferrimagnetic alignment of magnetic moments results in their alternating "up/down" arrangement along the [0 0 1] direction, as summarized in **Table 1**.

In order to investigate the magnetocaloric properties of $Mn_{2-x}Sn_{0.5}Ga_{0.5}$ alloys, we measured isothermal magnetization curves up to 30 kOe at various temperatures near their phase transitions. The existence of magnetic hysteresis during magnetization

Table 1 Calculated magnetic moments of $Mn_2Sn_{0.5}Ga_{0.5}$. For the numbering of Mn atoms, see Fig. 4.

m/atom (μ_B)	Mn1	Mn2	Mn3	Mn4	Ga	Sn	Total
$Mn_4Sn_1Ga_1$	−2.75	3.19	−2.75	3.19	0.01	0.01	0.90

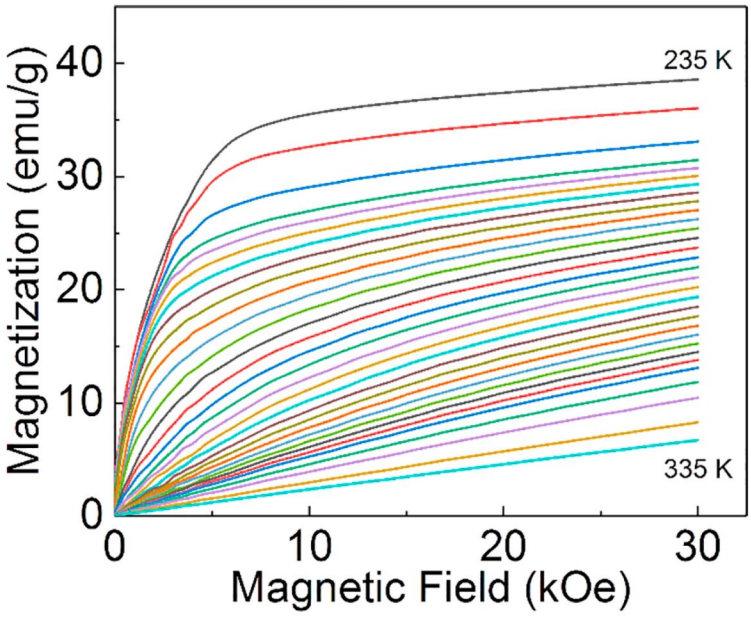

Fig. 5. Magnetization isotherms *M(H)* for magnetic fields up to 30 kOe at different temperatures for $Mn_{1.5}Sn_{0.5}Ga_{0.5}$ as-quenched ribbons.

and demagnetization of a sample is one of the major issues for magnetocaloric materials. Generally, hysteresis is a characteristic typical of materials showing first-order phase transition but other extrinsic factors such as impurities in the sample and lack of thermal equilibrium during measurement may also lead to a small hysteresis effect [34]. As an example, the *M(H)* plots for $Mn_{1.5}Sn_{0.5}Ga_{0.5}$ recorded between 235 K and 335 K are shown in **Fig. 5**. Since the hysteretic loss has a maximum value at the temperature of phase transition, we also recorded isothermal magnetization curve for $Mn_{1.5}Sn_{0.5}Ga_{0.5}$ at 276 K during magnetization and demagnetization of the sample and found a perfect reversibility of magnetic transition without a clear magnetic hysteresis. These isothermal magnetization curves were used to calculate the magnetic entropy change (ΔS_M) as a function of temperature.

In order to further understand the nature of phase transition in $Mn_{2-x}Sn_{0.5}Ga_{0.5}$ alloys, we plotted M^2 versus H/M (Arrott plots) for all samples and that for $Mn_{1.5}Sn_{0.5}Ga_{0.5}$ is shown in **Fig. 6**. As shown in Fig. 6, all the curves in the Arrott plot have a positive slope. Based on the Banerjee criterion, this observation confirms the second order

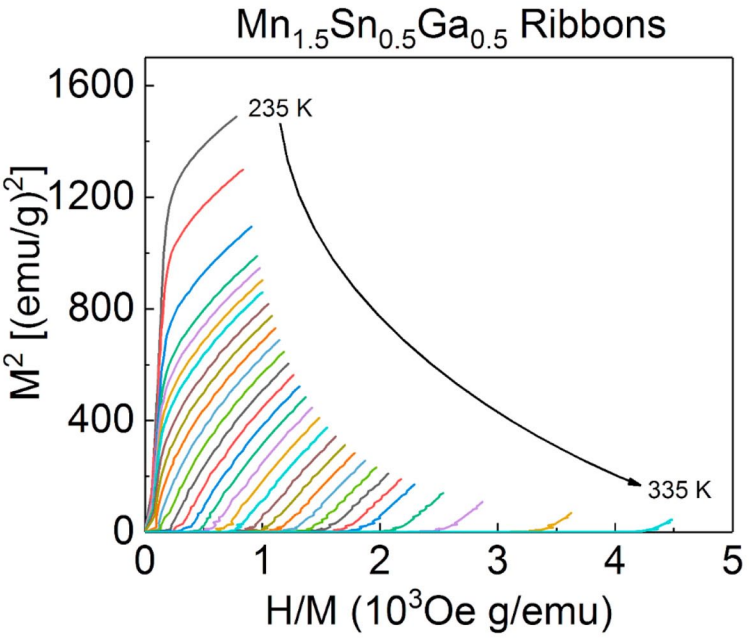

Fig. 6. Arrott plots (M_2 *vs. H/M*) for as-quenched $Mn_{1.5}Sn_{0.5}Ga_{0.5}$ ribbons.

nature of magnetic transition in this sample [35]. We have observed similar phase transitions in the other samples as well.

For a magnetocaloric material, the relative cooling power (RCP) is an important parameter which is generally calculated from the peak value of magnetic entropy change ($\Delta S_{M,max}$) using the expression $RCP = |\Delta S_{M,max}| \times \Delta T_{FWHM}$, where ΔT_{FWHM} is the full width at half maximum of $\Delta S_M(T)$ curve. These values are displayed as RCP-1 in **Table 2**. For comparison, we have also calculated the RCP values from the

Table 2 Magnetic properties of $Mn_{2-x}Sn_{0.5}Ga_{0.5}$ (x=0, 0.3, 0.5, 0.8) as-quenched ribbons.

Material	Curie Temperature (K)	Peak value of $-\Delta S_M$ (J/kgK) ΔH= 10 kOe	ΔH= 20 kOe	ΔH= 30 kOe	RCP-1 at 30 kOe ±0.9 (J/kg)	RCP-2 at 30 kOe (J/kg)
$Mn_{1.2}Sn_{0.5}Ga_{0.5}$	306	0.57	1.05	1.47	121.1	92.5
$Mn_{1.5}Sn_{0.5}Ga_{0.5}$	284	0.70	1.25	1.70	89.5	66.7
$Mn_{1.7}Sn_{0.5}Ga_{0.5}$	283	0.70	1.25	1.70	84.7	62.7
$Mn_2Sn_{0.5}Ga_{0.5}$	262	0.50	0.90	1.23	72.7	54.2

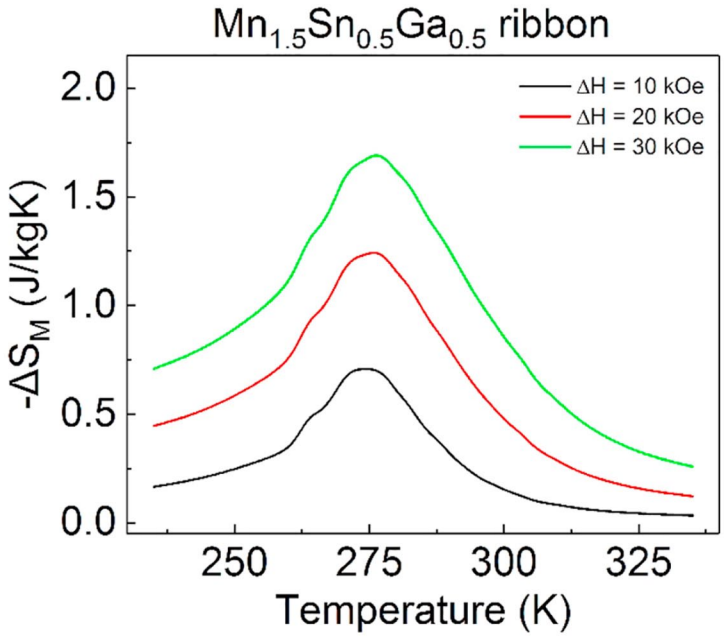

Fig. 7. Magnetic entropy change ($-\Delta S_M$) as a function of temperature for $Mn_{1.5}Sn_{0.5}Ga_{0.5}$ as-quenched ribbons.

integration of ΔS_M and displayed as RCP-2 in Table 2 [36]. We calculated ΔS_M for all samples at a field change of 10 kOe, 20 kOe and 30 kOe and at various temperatures between 235 K and 335 K using Maxwell's thermodynamic relation $S_M(T, H) = \int_0^H (dM/dT)_H dH$ [9]. **Fig. 7** shows $-\Delta S_M$ as a function of temperature near the phase-transition temperature of $Mn_{1.5}Sn_{0.5}Ga_{0.5}$ measured at the field change of 10 kOe, 20 kOe and 30 kOe. The peak value of ΔS_M occurred at 276 K which is close to its Curie temperature. As displayed in Table 2, all of the $Mn_{2-x}Sn_{0.5}Ga_{0.5}$ ribbons show relatively low values of $\Delta S_{M,max}$ with $Mn_{1.5}Sn_{0.5}Ga_{0.5}$ showing 1.7 J/KgK at 30 kOe. Zhao et al. have reported magnetocaloric properties of similar compound $Mn_5Sn_{3-x}Ga_x$ and found $\Delta S_{M,max}$ = 0.9 J/kgK at 20 kOe for $Mn_5Sn_{1.5}Ga_{1.5}$ with T_c of 282 K [37]. Zhang et al. measured $\Delta S_{M,max}$ of about 0.8 J/kgK at 20 kOe for $Fe_2MnSi_{0.5}Ge_{0.5}$ (T_c=260 K)[38]. Our measured value ($\Delta S_{M,max}$ =1.3 J/kgK) at 20 kOe for $Mn_{1.5}Sn_{0.5}Ga_{0.5}$ (T_c=284 K) is slightly higher than the values reported in Refs. [37] and [38]. The wide temperature range between the hot and cold side of the $\Delta S_M(T)$ curve has resulted in relatively high value of RCP.

4. Conclusions

$Mn_{2-x}Sn_{0.5}Ga_{0.5}$ (x=0, 0.3, 0.5, 0.8) alloys with a hexagonal crystal structure have been prepared using arc-melting and rapid quenching in a melt-spinner chamber. All samples show single magnetic phase transitions near room temperature. The Curie temperature and saturation magnetization are sensitive to Mn concentration in $Mn_{2-x}Sn_{0.5}Ga_{0.5}$, where both *Tc* and *Ms* decrease with the increase in Mn concentration indicating the existence of ferrimagnetic order in these materials. This is in qualitative agreement with first-principle calculations. All samples show relatively small values of entropy change but the relative cooling powers are comparable to other non-rare-earth materials exhibiting second order phase transitions. If the magnetizations of these materials can be increased by adjusting elemental composition or doping with other suitable elements, high entropy change at room temperature can be obtained. The use of non-toxic and inexpensive elements, lack of thermal and magnetic hysteresis with broad working temperature near room temperature makes these materials of interest for room-temperature magnetic refrigeration.

Acknowledgments This research is supported by Scholarly Excellence Funds, Office of Academic Affairs and Department of Physics, South Dakota State University. The research at University of Nebraska is supported by the USDOE under grant DE-FG02-04ER46152. The research was performed in part in the Nebraska Nanoscale Facility: National Nanotechnology Coordinated Infrastructure and in the Nebraska Center for Materials and Nanoscience, which are supported by the National Science Foundation under Award ECCS:1542182 and by the Nebraska Research Initiative. We would like to thank Bishnu Dahal for useful discussion.

References

[1] K.A. Gschneidner Jr., V.K. Pecharsky, A.O. Tsokol, Recent developments in magnetocaloric materials, Rep. Prog. Phys. 68 (2005) 1479–1539.

[2] B.G. Shen, J.R. Sun, F.X. Hu, H.W. Zhang, Z.H. Cheng, Recent progress in exploring magnetocaloric materials, Adv. Mater. 21 (2009) 4545–4564.

[3] M. Balli, S. Jandl, P. Fournier, A. Kedous-Lebouc, Advanced materials for magnetic cooling: fundamentals and practical aspects, Appl. Phys. Rev. 4 (2017) 021305.

[4] A. Planes, L. Manosa, M. Acet, Magnetocaloric effect and its relation to shapememory properties in ferromagnetic Heusler alloys, J. Phys.: Condens. Matter. 21 (2009) 233201.

[5] V. Franco, J.S. Blazquez, J.J. Ipus, J.Y. Law, L.M. Moreno-Ramirez, A. Conde, Magnetocaloric effect: from materials research to refrigeration devices, Prog. Mater. Sci. 93 (2018) 112–232.

[6] A.M. Tishin, Y.I. Spichkin, Recent progress in magnetocaloric effect: mechanisms and potential applications, Int. J. Refrig. 37 (2014) 223–229.

[7] A. Kitanovski, J. Tusek, U. Tomc, U. Plaznik, M. Ozbolt, A. Poredos, Magnetocaloric Energy Conversion: From Theory to Applications, Springer International Publishing, Cham, Switzerland, 2015.

[8] M. Phan, S. Yu, Review of the magnetocaloric effect in manganite materials, J. Magn. Magn. Mater. 308 (2007) 325–340.

[9] V.K. Pecharsky, K.A. Gschneidner Jr., Giant magnetocaloric effect in $Gd_5(Si_2Ge_2)$, Phys. Rev. Lett. 78 (1997) 4494–4497.

[10] S.Y. Dan'kov, A.M. Tishin, V.K. Pecharsky, K.A. Gschneidner Jr., Magnetic phase transitions and the magnetothermal properties of gadolinium, Phys. Rev. B 57 (1998) 3478–3490.

[11] B. Yu, M. Liu, P.W. Egolf, A. Kitanovski, A review of magnetic refrigerator and heat pump prototypes built before the year 2010, Int. J. Refrig. 33 (2010) 1029–1060.

[12] F. Hu, B. Shen, J. Sun, G. Wang, Z. Cheng, Very large magnetic entropy change near room temperature in $LaFe_{11.2}Co_{0.7}Si_{1.1}$, Appl. Phys. Lett. 80 (2002) 826–828.

[13] A. Fujita, S. Fujieda, Y. Hasegawa, K. Fukamichi, Itinerant-electron metamagnetic transition and large magnetocaloric effects in $La(Fe_xSi_{1-x})_{13}$ compounds and their hydrides, Phys. Rev. B 67 (2003) 104416.

[14] O. Tegus, E. Bruck, K.H.J. Buschow, F.R. de Boer, Transition-metal-based magnetic refrigerants for room-temperature applications, Nature 415 (2002) 150–152.

[15] D.T. Cam Thanh, E. Bruck, N.T. Trung, J.C.P. Klaasse, K.H.J. Buschow, Structure, magnetismand magnetocaloric properties of $MnFeP_{1-x}Si_x$ compounds, J. Appl. Phys. 103 (2008) 07B318.

[16] T. Krenke, E. Duman, M. Acet, E.F. Wassermann, X. Moya, L. Manosa, A. Planes, Inverse magnetocaloric effect in ferromagnetic Ni–Mn–Sn alloys, Nat. Mater. 4 (2005) 450–454.

[17] F. Hu, B. Shen, J. Sun, Magnetic entropy change in $Ni_{51.5}Mn_{22.7}Ga_{25.8}$ alloy, Appl. Phys. Lett. 76 (2000) 3460–3462.

[18] A.R. Dinesen, S. Linderoth, S. Morup, Direct and indirect measurement of the magnetocaloric effect in $La_{0.67}Ca_{0.33-x}Sr_xMnO_{3\pm\delta}$ ($x \in [0; 0.33]$), J. Phys.: Condens. Matter. 17 (2005) 6257–6269.

[19] Bishnu R. Dahal, Kyle Schroeder, Megan M. Allyn, Ronald J. Tackett, Yung huh and parashu kharel, near-room-temperature magnetocaloric properties of $La_{1-x}Sr_xMnO_3$, Mater. Res. Express 5 (2018) 106103.

[20] H. Baaziz, A. Tozri, E. Dhahri, E.K. Hlil, Magnetocaloric properties of $La_{0.67}Sr_{0.33}MnO_3$ tunable by particle size and dimensionality, Chem. Phys. Lett. 691 (2018) 355–359.

[21] R. Fuglsby, P. Kharel, W. Zhang, S. Valloppilly, Y. Huh, D.J. Sellmyer, Magnetism of hexagonal $Mn_{1.5}X_{0.5}Sn$ (X = Cr, Mn, Fe, Co) nanomaterials, J. Appl. Phys. 117 (2014) 17D115.

[22] K. Schroeder, J. Waybright, P. Kharel, W. Zhang, S. Valloppilly, J. Herran, P. Lukashev, Y. Huh, R. Skomski, D.J. Sellmyer, Magnetic and magnetocaloric properties of $Co_{2-x}Fe_xVGa$ Heusler alloys, AIP Adv. 8 (2018) 056431.

[23] S. Singh, L. Caron, S.W. D'Souza, T. Fichtner, G. Porcari, S. Fabbrici, C. Shekhar, S. Chadov, M. Solzi, C. Felser, Large magnetization and reversible magnetocaloric effect at the second-order magnetic transition in heusler materials, Adv. Mater. 28 (2016) 3321–3325.

[24] E. Bruck, O. Tegus, D.T. Cam Thanh, Nguyen T. Trung, K.H.J. Buschow, A review on Mn based materials for magnetic refrigeration: structure and properties, Int. J. Refrig. 31 (2008) 763–770.

[25] K.H.J. Buschow, P.G. van Engen, R. Jongebreur, Magneto-optical properties of metallic ferromagnetic materials, J. Magn. Magn. Mater. 38 (1983) 1–22.

[26] J. Winterlik, B. Balke, G.H. Fecher, C. Felser, M.C.M. Alves, F. Bernardi, J. Morais, Structural, electronic, and magnetic properties of tetragonal $Mn_{3-x}Ga$: experiments and first-principles calculations, Phys. Rev. B 77 (2008) 054406.

[27] L. Zhang, M. Bao, Q. Zheng, L. Tian, J. Du, Magnetocaloric effect in high Gd content Gd-Fe-Al based amorphous/nanocrystalline systems with enhanced curie temperature and refrigeration capacity, AIP Adv. 6 (2016) 035220.

[28] D.C. Jiles, Recent advances and future directions in magnetic materials, Acta Mater. 51 (2003) 5907–5939.

[29] Kō Yasukōchi, Kazuo Kanematsu, Tetuo Ohoyama, Magnetic properties of intermetallic compounds in manganese-Tin system: $Mn_{3.67}Sn$, $Mn_{1.77}Sn$, and $MnSn_2$, J. Phys. Soc. Jpn. 16 (1961) 1123–1130.

[30] P. Blochl, Projector augmented-wave method, Phys. Rev. B 50 (1994) 17953–17979.

[31] G. Kresse, D. Joubert, From ultrasoft pseudopotentials to the projector augmentedwave method, Phys. Rev. B 59 (1999) 1758–1775.

[32] J.P. Perdew, K. Burke, M. Ernzerhof, Generalized gradient approximation made simple, Phys. Rev. Lett. 77 (1996) 3865–3868.

[33] M. Methfessel, A.T. Paxton, High-precision sampling for Brillouin-zone integration in metals, Phys. Rev. B 40 (1989) 3616–3621.

[34] F.X. Hu, L. Chen, J. Wang, L.F. Bao, J.R. Sun, B.G. Shen, Particle size dependent hysteresis loss in $La_{0.7}Ce_{0.3}Fe_{11.6}Si_{1.4}C_{0.2}$ first order systems, Appl. Phys. Lett. 100 (2012) 072403.

[35] B.K. Banerjee, On a generalised approach to first and second order magnetic transitions, Phys. Lett. 12 (1964) 16–17.

[36] Pedro Gorria, Jose L. Sanchez Llamazares, Pablo Alvarez, Maria Jose Perez, Jorge Sanchez Marcos, Jesus A. Blanco, Relative cooling power enhancement in magnetocaloric nanostructured Pr_2Fe_{17}, J. Phys. D: Appl. Phys. 41 (2008) 192003.

[37] F.Q. Zhao, W. Dagula, O. Tegus, T.J. Gortenmulder, E. Bruck, K.H.J. Buschow, Magnetocaloric properties of $Mn_5Sn_{3-x}Ga_x$ alloys, IEEE Trans. Magn. 41 (2005) 3754–3756.

[38] L. Zhang, E. Bruck, O. Tegus, K.H.J. Buschow, F.R. de Boer, The crystallographic phases and magnetic properties of $Fe_2MnSi_{1-x}Ge_x$, Physica B 328 (2003) 295–301.